

**FULL PAPER**

# Guanine-La complex supported onto SBA-15: A novel efficient heterogeneous mesoporous nanocatalyst for one-pot, multi-component Tandem Knoevenagel condensation–Michael addition–cyclization Reactions

Mohsen Nikoorazm | Maryam Khanmoradi | Masoud Mohammadi

Department of Chemistry, Faculty of Science, Ilam University, P. O. Box 69315516, Ilam, Iran

**Correspondence**

Mohsen Nikoorazm; Department of Chemistry, Faculty of Science, Ilam University, P.O. Box 69315516 Ilam, Iran.  
Email: e\_nikoorazm@yahoo.com

In this work, we present a simple, environmentally-friendly and economical route for the preparation of a novel lanthanum (III) organometallic complex immobilized onto a highly stable mesoporous silica SBA-15 (La-guanine@SBA-15) using an inexpensive and simple method and available materials. This mesoporous heterogenized complex was comprehensively characterized using FT-IR, XRD, EDS, ICP, MAP, SEM, TGA and BET techniques. The catalytic activity of this mesoporous material was studied in one-pot multi-component tandem Knoevenagel condensation–Michael addition–cyclization reactions in order to prepare a series of benzo [a] pyrano [2, 3-c] phenazine and 4,4'-(arylmethylene)-bis-(3-methyl-1-phenyl-1H-pyrazol-5-ols) derivatives under green conditions. This catalyst exhibited highly recoverable and recyclable features in consecutive reaction runs. Besides, the products were obtained in high yields and short reaction times. In this sense, simple preparation of the catalyst from the commercially available materials, simple operation, high catalytic activity, short reaction times, high yields and the use of green reaction conditions in the mentioned organic synthesis are the most significant advantages of this protocol. In addition, this nanocatalyst was easily recovered, using simple filtration, and reused several times without significant loss of its catalytic efficiency. Moreover, the leaching, heterogeneity and stability of La-guanine@SBA-15 were studied by hot filtration test and ICP technique. Finally, stability of the catalyst after recycling was confirmed by SEM and FT-IR techniques.

**KEYWORDS**

4,4'-(arylmethylene)-bis-(3-methyl-1-phenyl-1H-pyrazol-5-ols), Benzo [a] pyrano [2, 3-c] phenazines, La-guanine@SBA-15, mesoporous nanocatalyst, Tandem Knoevenagel condensation–Michael addition–cyclization

**1 | INTRODUCTION**

Over the past decade, the field of synthetic chemistry has witnessed the multicomponent reactions (MCRs)

renaissance as a powerful method for the preparation of products in a single-step and synthetic operation with high efficiency.<sup>[1,2]</sup> MCRs comprise an important class of chemical transformations which has been applied to

almost all fields of organic and medicinal chemistry.<sup>[3,4]</sup> Tandem or domino (cascade) reactions consist of two or more successive independent reactions performed in a one-pot system without separating and purifying the intermediates.<sup>[5–7]</sup> These convergent procedures incorporate three or more reactants into the final product in just one pot. Thus, they can combine high levels of complex and diverse generations with low synthetic cost and high atom-economy and also reduce the waste generation and synthetic efficiency.<sup>[8–10]</sup> Consequently, tandem reactions not only reduce the number of reaction steps, energy consumption and waste but also minimize the use of solvents and reagents.<sup>[11]</sup> These advantages make tandem reactions sustainably green processes that illustrate the concepts of efficiency and atom economy.<sup>[11–13]</sup> Tandem reactions offer many opportunities to improve chemical transformations such as Lewis acid–base catalysis, hydrogenation reactions and alkene metathesis.<sup>[14,15]</sup> MCRs are currently well-established methods for the synthesis of heterocycles,<sup>[16–19]</sup> natural products<sup>[13,20,21]</sup> and polymers<sup>[22,23]</sup> while Double and Triple Cascade Reactions are still a growing field of research. Knoevenagel condensation–Michael addition (Double Cascade Reactions) and Knoevenagel condensation–Michael addition–cyclization (Triple Cascade Reactions) Sequences have been widely studied and frequently applied to the synthesis of natural products and biologically active compounds.<sup>[15,24]</sup> These methods are highly valuable for the formation of chiral carbo- and heterocyclic compounds with multiple stereocenters which are relevant to the pharmaceutical and medicinal chemistry and useful in the synthesis of various natural products.<sup>[14,15,25–30]</sup>

Benzo [a] pyrano [2, 3-c] phenazine and 4,4'-(arylmethylene)-bis-(3-methyl-1-phenyl-1H-pyrazol-5-ols) compounds have a great potential in order to be applied in biological and pharmaceutical systems such as antifungal, anticancer, antiplasmodial, antimalarial, antibacterial, antiparasitic, anticancer and antichagasas systems.<sup>[27,28,31–39]</sup> However, synthesis of these useful compounds needs a better method which should be in agreement with green chemistry rules.

Mesoporous materials are interesting materials having highly ordered pores and a large surface area. Besides, they are widely applied in catalysis as catalyst supports, separations, adsorption, gas sensors and drug delivery systems.<sup>[40–43]</sup> After the discovery of mesoporous silica structures in the early 1990s, various types of these materials, such as MCM (Mobil Crystalline Material), MSU (Michigan State University) and SBA (Santa Barbara Amorphous), have been developed.<sup>[42,44,45]</sup> Noticeably, different types of surfactants, pH, temperature, time, etc. can significantly change the material properties and produce different types of mesoporous

materials i.e. increasing the temperature and time which leads to increase the pore size and decreases the specific surface area.<sup>[46]</sup> Moreover, the solvent which can be used for washing prior to the calcinations in the synthesis of SBA-15 can be a crucial step because different washing procedures per washing cycle of SBA-15 surface (solvent volume and types of solvents) led to different porosity values/characteristics.<sup>[43]</sup>

Therefore, we can change characteristics of SBA-15 to desirable features. Based on the pore types, various mesoporous structures have been classified into three categories: 1) nearly spherical cage 2) bi-continuous channel and 3) cylindrical channel.<sup>[47]</sup> During the last decade, numerous efforts have been devoted to the catalytic reforming technology and obtaining molecular sieves showing larger pore size. Besides, it is worth mentioning that a permanent effort has also been made in order to develop textured inorganic or hybrid phases. More recently, SBA-15 was used as a promising inorganic support due to its structural properties and various technological applications such as molecular sieves, sensors, catalysts, nanoelectronics, drug delivery and separation.<sup>[48–54]</sup> Recent studies have demonstrated that several factors can control the condensation rates of SBA-15 which contains amounts of inorganic salts, shape of surfactant micelles, stirring rate and condensation rate of silica.<sup>[55]</sup> On the other hand, metal–organic complexes, involving rare earth elements such as lanthanide ions, are often used in catalysis field because they have the oxophilic nature and can easily build a framework structure.<sup>[14,56–60]</sup>

Herein, we describe the synthesis of an efficient and reusable catalyst by the immobilization of a lanthanum (III) complex with guanine as a coordinate ligand on chloro-functionalized SBA-15 mesoporous silica nanoparticles and its catalytic activities for one-pot synthesis of domino of benzo [a] pyrano [2, 3-c] phenazine and 4,4'-(arylmethylene)-bis-(3-methyl-1-phenyl-1H-pyrazol-5-ols) derivatives. The results of this study differ from the previously-reported researches due to the natural origin of ligand, stable complex of ligand with La and support, high yields of products and excellent selectivity and recoverability and reusability of the catalyst. In addition, ethanol was utilized as a green solvent under aerobic reaction conditions.

## 2 | EXPERIMENTAL

### 2.1 | Synthesis of La-guanine@SBA-15

In a typical synthesis, 4 g of the nonionic surfactant (Pluronic P123: EO<sub>20</sub>PO<sub>70</sub>EO<sub>20</sub>) was dissolved under

stirring in a solution containing water and 2 M HCl (90 ml) at 35 °C until the solution became homogeneous. Then, 9.04 ml of the silica precursor (TEOS: tetraethylorthosilicate) was slowly added to the reaction mixture and, then, the stirring continued for another 20 hr. Subsequently, the white solid product was filtered and washed with deionized water several times which can be regarded as a critical step before the final calcination aimed at removing the surfactant (P123) 35. After washing, the product was dried at 80 °C and the surfactant was removed by calcination at 823 K for 5 hr at a rate of 2 °C/min.

In order to functionalize mesoporous SBA-15, 1 g of the purely obtained SBA-15 was transferred into a clean flask, containing 20 ml n-hexane and 1.5 ml 3-chloropropyltriethoxysilane (nPrCl), and refluxed for 24 hr. After completion of the reaction, the resulting mixture was separated by simple filtration, washed with n-hexane and dried at 40 °C for 4 hr.

Continuously, 0.5 g of the Cl-functionalized SBA-15 was mixed with 0.181 g guanine (2-amino-1H-purin-6(9H)-one) (1.2 mmol) in toluene and refluxed at 120 °C under nitrogen atmosphere for 24 hr. Then, the obtained guanine@SBA-15 product was separated by simple filtration, washed with ethanol in order to remove the unreacted nucleobase and dried in an oven at 60 °C for 4 hr.

Finally, in order to prepare the La-guanine@SBA-15 heterogenized complex, 0.5 g of the synthesized guanine@SBA-15, in the previous step, reacted with La (NO<sub>3</sub>)<sub>3</sub>·6H<sub>2</sub>O (1.5 mmol, 0.649 g) in ethanol under reflux conditions for 20 hr. Ultimately, the obtained product was separated by simple filtration, washed with ethanol and water to remove the excess La, and dried in an oven at 80 °C for 4 hr.

## 2.2 | General pathway for the synthesis of benzo [a] pyrano [2, 3-c] phenazine derivatives

A mixture of 2-hydroxynaphthalene-1,4-dione (1 mmol) and benzene-1,2-diamine (1 mmol) was dissolved in 10 ml EtOH. Then, La-guanine-SBA-15 (0.5 mol%) was added to the mixture, and the flask was sealed and stirred at 80 °C under reflux conditions. The progress of the reaction was monitored by TLC. Upon the completion of the first step of the reaction, aromatic aldehyde (1.0 mmol) and malononitrile (1.5 mmol) were added into the reaction mixture and stirred for an appropriate time at reflux conditions. After completion of the reaction (monitored by TLC (n-hexane/ethyl acetate: 7/3), the mixture was cooled down to room temperature, filtered

and washed with hot acetone and, then, the catalyst was separated from other materials (the reaction mixture was soluble in hot acetone and the catalyst was insoluble). Afterwards, the solvent removal was carried out and, for further purification, the crude product was recrystallized in ethanol.

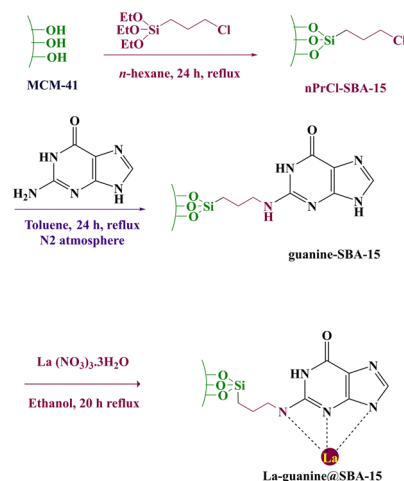
## 2.3 | General pathway for the synthesis of 4,4'-(arylmethylene)-bis-(3-methyl-1-phenyl-1H-pyrazol-5-ols)

A mixture of aldehyde (1 mmol), 3-Methyl-1-phenyl-5-pyrazolone (2 mmol) and La-guanine-SBA-15 (0.5 mol%) was dissolved in 3 ml EtOH. Then, the flask was sealed and stirred at 80 °C under reflux conditions. The progress of the reaction was monitored by TLC (n-hexane/ethyl acetate: 4/1). After completion of the reaction, the mixture was cooled down to room temperature, filtered and washed with hot EtOH to separate the catalyst from other materials (the reaction mixture was soluble in hot EtOH and the solid catalyst was insoluble). Finally, the solvent removal was carried out and, for further purification and to yield the pure products, the crude product was recrystallized by ethanol.

## 3 | RESULTS AND DISCUSSION

### 3.1 | Catalyst preparation

The presented work tries to describe a novel La-guanine Complex supported onto mesoporous SBA-15 as an efficient and green nanocatalyst for multicomponent organic



**SCHEME 1** Synthesis of La@guanine@SBA-15 nanostructure [Colour figure can be viewed at [wileyonlinelibrary.com](http://wileyonlinelibrary.com)]

transformations. Initially, the SBA-15 nanoparticles which were modified by immobilization of CPTMS on its surface (CPTMS@SBA-15) have been prepared according to our previously reported procedure.<sup>[14]</sup> In order to prepare guanine@SBA-15 NPs, 2-Amino-1,7-dihydro-6H-purin-6-one (guanine) has been grafted on CPTMS@SBA-15 NPs via the substitution reaction of  $\text{NH}_2$  with terminal Cl groups. Finally, the catalyst was synthesized by the reaction of guanine@SBA-15 with lanthanum (III) nitrate (Scheme 1).

### 3.2 | Catalyst characterizations

The prepared La-guanine@SBA-15 heterogeneous catalyst was also characterized by Fourier transform infrared spectroscopy (FT-IR), X-Ray Diffractometer (XRD), energy-dispersive X-ray spectroscopy (EDS), inductively coupled plasma atomic emission spectroscopy (ICP), X-ray mapping, scanning electron microscopy (SEM),

thermogravimetric analysis (TGA) and Brunauer–Emmett–Teller (BET) techniques.

The FT-IR spectra of the parent SBA-15 (a) nPrCl-SBA-15 (b), guanine-SBA-15 (c) and La@guanine@SBA-15 (d) are shown in Figure 1. Considering SBA-15, the present bands at about  $1082\text{ cm}^{-1}$ ,  $807\text{ cm}^{-1}$  and  $462\text{ cm}^{-1}$  attributed to the vibration modes of asymmetric stretching, symmetric stretching and bending Si-O-Si.<sup>[14,61,62]</sup> The presence of hydroxyl groups is well seen at  $3443\text{ cm}^{-1}$  (Figure 1 (a)).<sup>[14,63]</sup> In Figure 1 (b), the characteristic band at around  $2935\text{ cm}^{-1}$  is duo to  $\text{CH}_2$  vibrations corresponding to the C-H stretching and confirming the successful chloro-functionalization of SBA-15.<sup>[14,64]</sup> In Figure 1 (c) the band at  $1678\text{ cm}^{-1}$  and  $1588\text{ cm}^{-1}$  can be attributed to C=N and aromatic C-C groups on the guanine ring.<sup>[58]</sup> In Figure 1 (d), the band corresponding to N-H stretching vibrations ( $2983\text{ cm}^{-1}$ ) displays a small shift to the higher frequency ( $3012\text{ cm}^{-1}$ ) that can be due to the N group coordination of the guanine ring to the La metal.<sup>[14,58]</sup>

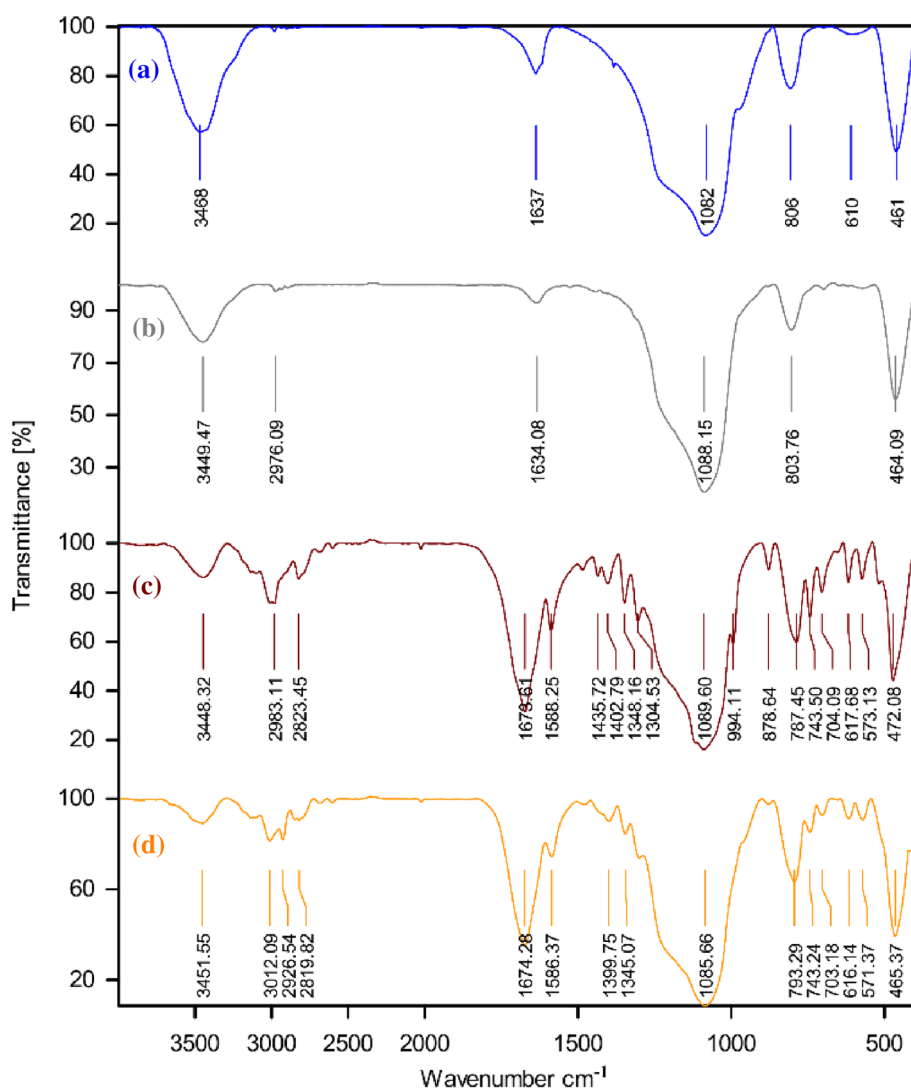


**FIGURE 1** FT-IR spectra of (a) SBA-15, (b) nPrCl-SBA-15, (c) guanine-SBA-15 and (d) La@guanine@SBA-15 [Colour figure can be viewed at [wileyonlinelibrary.com](http://wileyonlinelibrary.com)]

Figure 2. shows the low-angle XRD pattern of La@guanine@SBA-15. The lattice parameter on SBA-15 which can be indexed as the (100), (110), (200) reflections corresponds to p6mm space group of the two-dimensional hexagonal lattice.<sup>[47,65,66]</sup> Decreasing in the diffraction intensity of these three peaks for the catalyst indicated successful formation of La complex in the SBA-15 hexagonal channels. Thus far, only one well-resolved peak at  $2\theta \approx 1.20^\circ$  ( $d_{100}$ ) can be recognized and the ( $d_{110}$ ) and ( $d_{200}$ ) reflections disappeared. Also, it was found that the position of the  $d_{100}$  peak in the catalyst shifted to lower values, which are due to the shrinking pore size, and reduced the order of homogeneity of the pores in comparison to SBA-15. This may correspond to the recondensation reactions of the silica with lanthanum nanoparticles in the pore channel.<sup>[46,62,65–67]</sup>

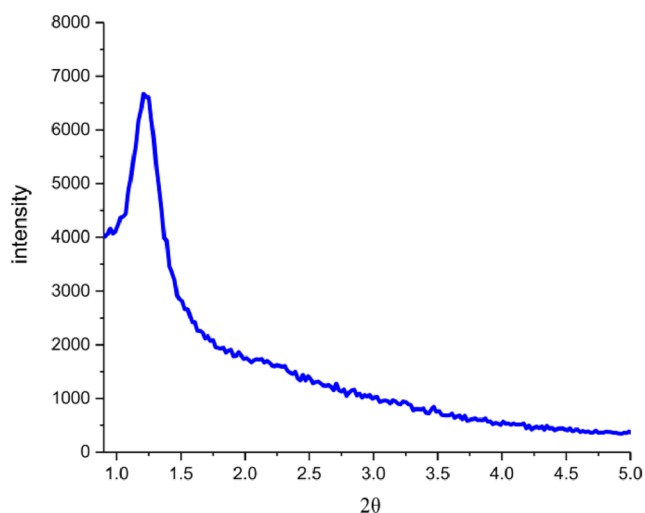


**FIGURE 2** The low-angle XRD pattern of La@guanine@SBA-15 [Colour figure can be viewed at [wileyonlinelibrary.com](#)]

Moreover, energy dispersive X-ray spectroscopy (EDS) analysis of La@guanine@SBA-15 is carried out to indicate the adsorption of  $\text{La}^{3+}$  on SBA-15 surface. These results are presented in Figure 3. In EDS image, the peaks associated with Si, O, C, N and La can be observed. It is found that the adsorption of lanthanum complex on SBA-15 surface was successfully performed. In addition, the exact amount of La, which was immobilized on guanine@SBA-15, was obtained by ICP-OSE as  $1.33 \times 10^{-3} \text{ mol g}^{-1}$ . Finally, in order to find the exact of carbon and nitrogen in the described catalyst, elemental analysis has been performed. Accordingly, the amounts of carbon and nitrogen immobilized on SBA-15 NPs were found to be 24.1 and 11.3, % respectively.

The X-ray mapping of La@guanine@SBA-15 was studied in order to explore the dispersion of all elements of the catalyst. As shown in Figure 4, the elemental map images illustrated good dispersion of La on La@guanine@SBA-15 surface and also showed that most of the particles are quasi-spherical.

Scanning electron microscopy (SEM) images of La@guanine@SBA-15 are shown in Figure 5 in which small particles' size and uniform morphology can be observed illustrating the vermicular-shaped particles in nanometer size.

The thermogravimetric analysis (TGA) was used to explore the presence of organic functional groups chemisorbed onto the SBA-15 heterogeneous surfaces. As shown in Figure 6, the thermogravimetric analysis (TGA) curves of La@guanine@SBA-15 are located in the following temperature ranges: from 100–300 °C due to the removal of physically adsorbed water and organic solvents,<sup>[14,58]</sup> from 300–350 °C and 350–650 as related to P123 decomposition and decomposition of other maintained functional organic groups chemisorbed onto the surface of SBA-15 nanoparticles.<sup>[14]</sup>

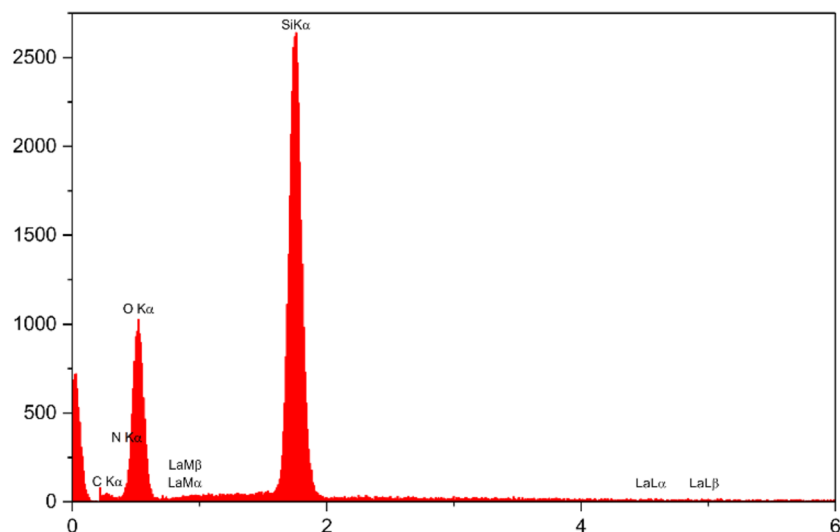


**FIGURE 3** The EDS spectrum of La@guanine@SBA-15 [Colour figure can be viewed at [wileyonlinelibrary.com](#)]

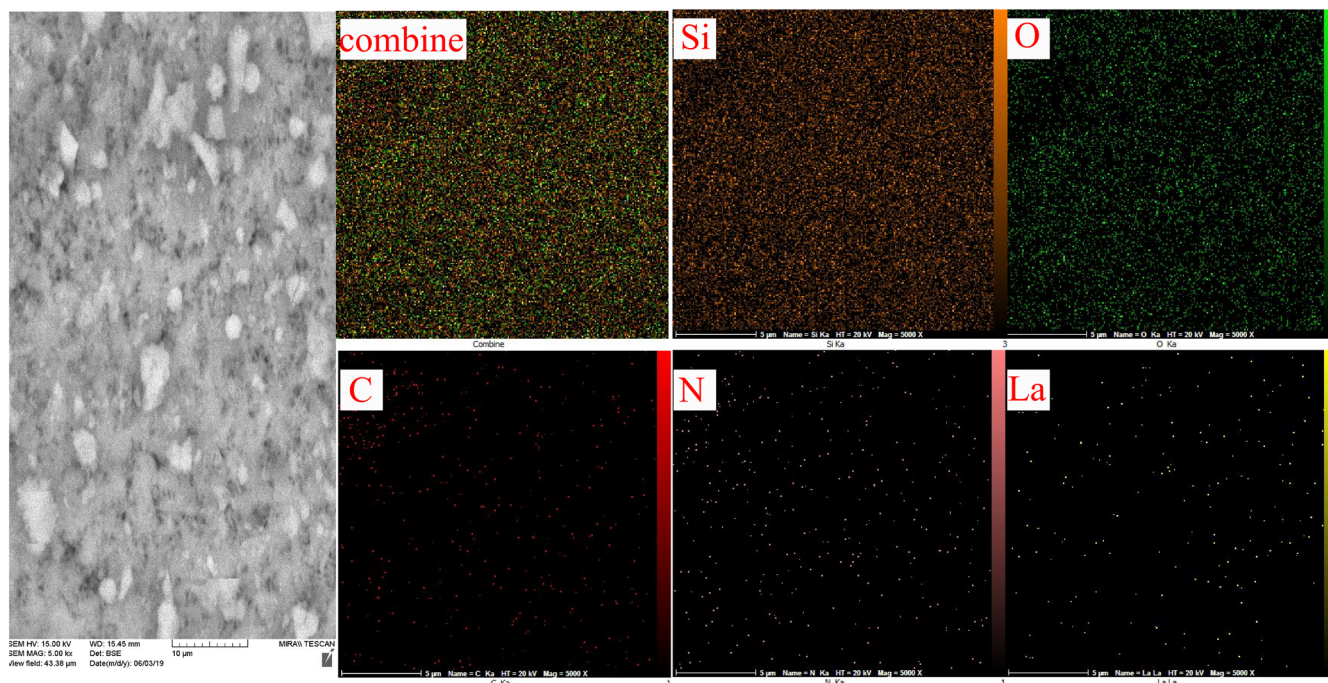


**FIGURE 4** The Map analysis of La@guanine@SBA-15 [Colour figure can be viewed at [wileyonlinelibrary.com](http://wileyonlinelibrary.com)]

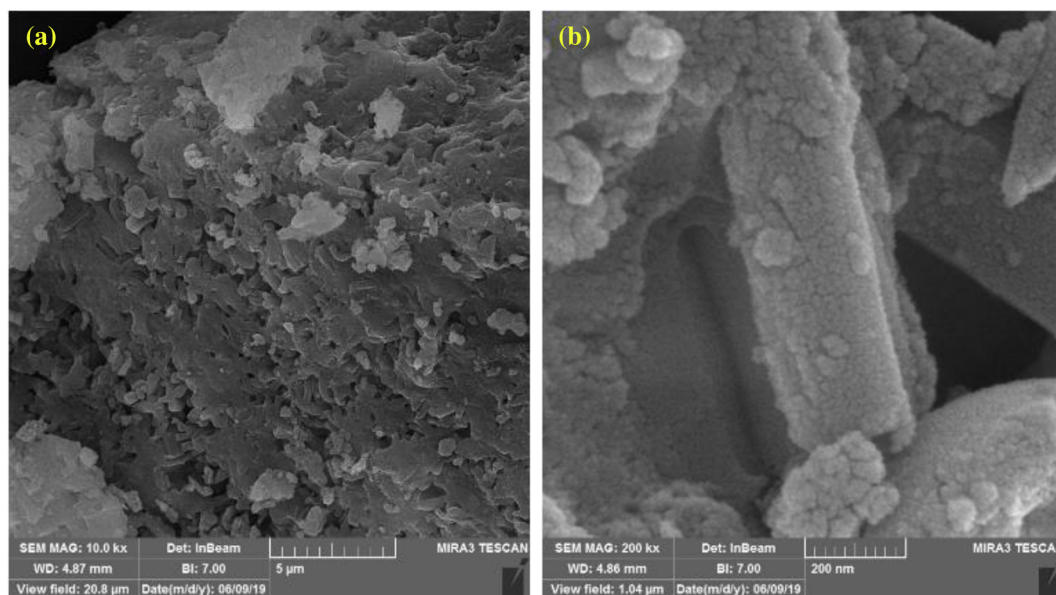


**FIGURE 5** SEM images of La@guanine@SBA-15 nanostructure [Colour figure can be viewed at [wileyonlinelibrary.com](http://wileyonlinelibrary.com)]

Textural parameters of La@guanine@SBA-15 were determined by nitrogen adsorption/desorption isotherms that illustrate type IV isotherm with an H1-type hysteresis loop at a relative pressure between 0.4–1.0, corresponding to mesoporous materials (Figure 7). The amounts of surface area, pore volume and pore size distribution of La@guanine@SBA-15 were determined by applying the Brunauer–Emmett–Teller (BET)

method and Barrett–Joyner–Halenda (BJH) models and, then, collected in Table 1. The values of these parameters are much lower as compared to that of the SBA-15 mesoporous.<sup>[14,61,65,68]</sup> This can be due to the fact that these value parameters which are closely related to the complex loading confirmed the successful incorporation of metal nanoparticles on SBA-15 heterogeneous surfaces.

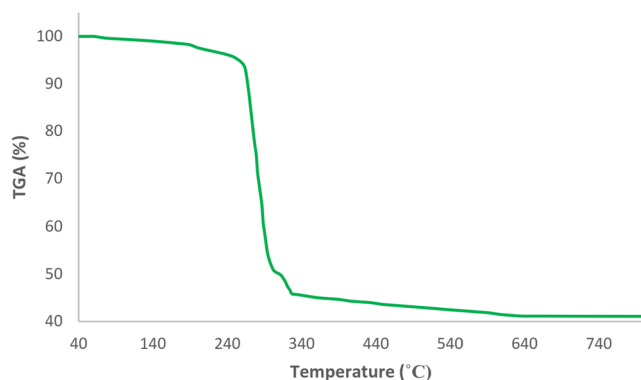


**FIGURE 6** TGA curves of La@guanine@SBA-15 [Colour figure can be viewed at wileyonlinelibrary.com]

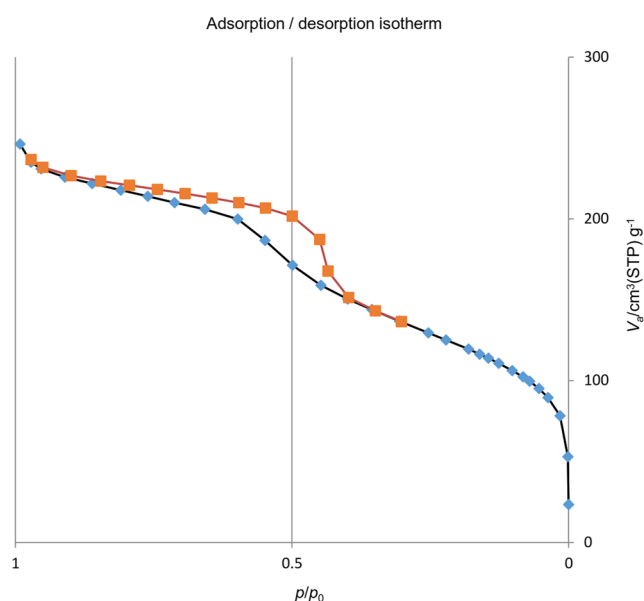


**FIGURE 7** Adsorption/Desorption isotherm of La@guanine@SBA-15 [Colour figure can be viewed at wileyonlinelibrary.com]

#### 4 | EVALUATION OF THE CATALYTIC ACTIVITY OF LA@GUANINE@SBA-15

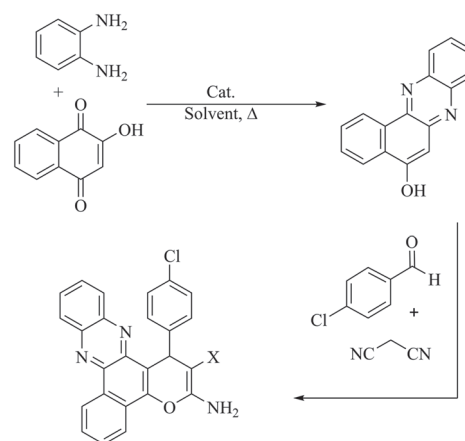
In continuation of our previous researches,<sup>[14,15]</sup> we wish to report a facile, efficient, and environmentally-friendly process for the preparation of benzo [a] pyrano [2, 3-c] phenazine and 4,4'-(arylmethylene)-bis-(3-methyl-1-phenyl-1H-pyrazol-5-ols) derivatives under green reaction

conditions in the presence of catalytic amount of La-guanine-SBA-15 mesoporous nanoparticles.

In catalytic studies, initially, the catalytic activity of La@guanine@SBA-15 is examined for the synthesis of benzo [a] pyrano [2, 3-c] phenazine derivatives by the reaction of benzene-1,2-diamine, 2-hydroxynaphthalene-1,4-dione, aldehydes and malononitrile. According to scheme 2, this was a one-pot and two-step procedure.

In this sense, the Schiff base condensation reaction between 2-hydroxynaphthalene-1,4-dione (1 mmol) and benzene-1,2-diamine (1 mmol) in the first step and 4-chlorobenzaldehyde (1 mmol) and malononitrile (1.5 mmol) in the second step were selected as the model reaction. The influence of effective parameters was also examined.

Examining the effect of various amounts of the catalyst was the first step of our optimization. The results in Table 2 showed that in the absence of a catalyst, no product was obtained after 48 hr (Table 2, entry 1) and the yield of the product was improved with increasing the amount of the catalyst (Table 2, entries 5–11). Therefore, the best result was obtained in the presence of 0.5 mol% of the catalyst on the basis of La. Next, we have successfully exploited the effect of several solvents; including, ethanol, water, ethanol:water, THF, PEG-400, DMF, DMSO, acetone, *n*-hexane Acetonitrile and solvent-free conditions (Table 2, entries 13–22) and also various temperatures in the range of 25 °C to reflux



**SCHEME 2** Optimization of reaction conditions for the Preparation of 3-Amino-1-(4-chloro-phenyl)-1H-benzo[a]pyrano [2,3-c]phenazine-2-carbonitrile in the presence of La@guanine@SBA-15 catalyst

**TABLE 1** Surface properties of La@guanine@SBA-15

Sample	$S_{\text{BET}}$ ( $\text{m}^2/\text{g}$ )	Pore diam. By BJH method (nm)	Pore vol. ( $\text{cm}^3/\text{g}$ )
La@guanine@SBA-15	430.22	3.526	0.3793

**TABLE 2** Optimization of reaction conditions for the Preparation of 3-Amino-1-(4-chloro-phenyl)-1H-benzo[a]pyrano [2,3-c] phenazine-2-carbonitrile in the presence of La@guanine@SBA-15 catalyst

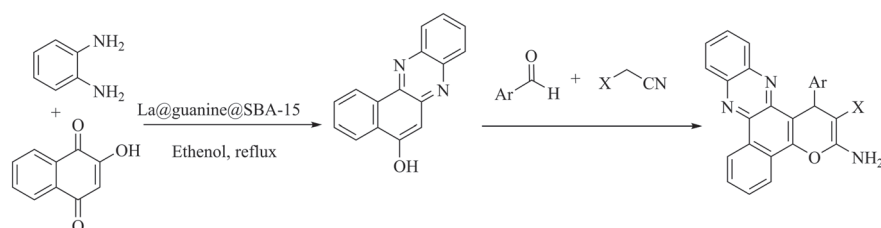
Entry	Catalyst	Amount of Catalyst (mol %)	Solvent	Temperature (°C)	Time (min)	Yield <sup>a</sup> (%)
1	-	-	Ethanol	Reflux	2 day	Trace
2	Guanine	0.5	Ethanol	Reflux	60	35
3	SBA-15	30 mg	Ethanol	Reflux	60	Trace
4	guanine@SBA-15	30 mg	Ethanol	Reflux	60	Trace
5	La (NO <sub>3</sub> ) <sub>3</sub> ·6H <sub>2</sub> O	0.5	Ethanol	Reflux	60	47
6	La@guanine@SBA-15	0.05	Ethanol	Reflux	60	Trace
7	La@guanine@SBA-15	0.1	Ethanol	Reflux	60	57
8	La@guanine@SBA-15	0.2	Ethanol	Reflux	60	70
9	La@guanine@SBA-15	0.3	Ethanol	Reflux	60	83
10	La@guanine@SBA-15	0.4	Ethanol	Reflux	60	91
11	La@guanine@SBA-15	0.5	Ethanol	Reflux	60	98
12	La@guanine@SBA-15	0.5	THF	100	60	70
13	La@guanine@SBA-15	0.5	Water	100	60	71
14	La@guanine@SBA-15	0.5	Ethanol: Water (1:1)	Reflux	60	76
15	La@guanine@SBA-15	0.5	Ethanol: Water (2:1)	Reflux	60	83
16	La@guanine@SBA-15	0.5	PEG-400	100	60	81
17	La@guanine@SBA-15	0.5	DMF	100	60	64
18	La@guanine@SBA-15	0.5	DMSO	100	60	71
19	La@guanine@SBA-15	0.5	Acetone	Reflux	60	37
20	La@guanine@SBA-15	0.5	<i>n</i> -hexane	Reflux	60	Trace
21	La@guanine@SBA-15	0.5	Solvent-free	100	60	65
22	La@guanine@SBA-15	0.5	Solvent-free	120	60	71
23	La@guanine@SBA-15	0.5	Ethanol	25	60	N.R
24	La@guanine@SBA-15	0.5	Ethanol	40	60	37
25	La@guanine@SBA-15	0.5	Ethanol	50	60	57
26	La@guanine@SBA-15	0.5	Ethanol	60	60	73
27	La@guanine@SBA-15	0.5	Ethanol	70	60	84

<sup>a</sup>Isolated yield.

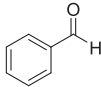
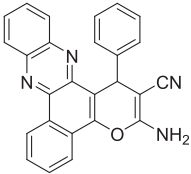
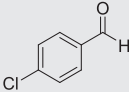
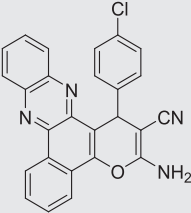
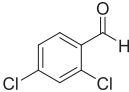
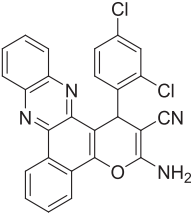
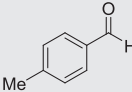
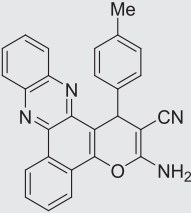
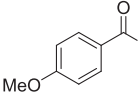
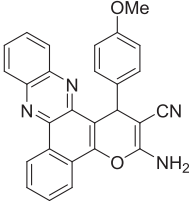
(Table 2, entries 11, 23–27). The obtained result showed that the reaction rate was strongly influenced by the type of solvent nature and temperatures. The reaction did not proceed in ethanol at 25 °C (Table 2, entry 11) and the best result was achieved in ethanol at reflux condition (Table 2, entry 5). For other solvents no

further improvement in the product yield was observed even at higher temperatures (100 °C).

In order to recognize the applicability of our procedure, the reaction scope was explored using various aldehydes with several functionalities such as F, Cl, CH<sub>3</sub>, NO<sub>2</sub> and OCH<sub>3</sub> under the optimized reaction conditions

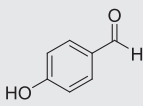
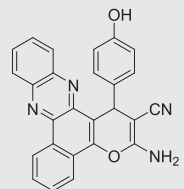
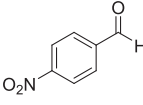
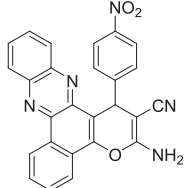
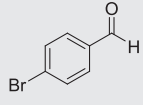
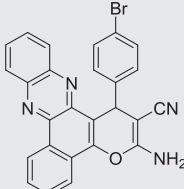
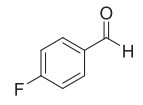
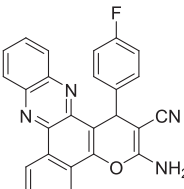
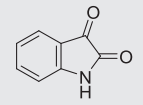
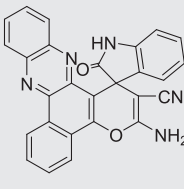
**SCHEME 3** One-pot, domino, multicomponent synthesis of benzo[c]pyrano[3,2-a]phenazine derivatives in the presence of La@guanine@SBA-15

**TABLE 3** One pot, domino, multi component synthesis of benzo[*c*]pyrano[3,2-*a*]phenazine derivatives using La@guanine@SBA-15 (50 mg) in ethanol at reflux condition

Entry	Aldehyde	Product	Time (h)	Yield <sup>a</sup> (%)	TON	TOF(h <sup>-1</sup> )	M.P °C	
							Measured	Literature
1			4	93	186	46.5	288–290	288–291 <sup>[25]</sup>
2			3	98	196	65.33	286–288	286–288 <sup>[69]</sup>
3			3	99	198	66	308–310	307–310 <sup>[69]</sup>
4			5	90	180	36	295–298	295 <sup>[69]</sup>
5			4.5	95	190	42.22	274–275	273 <sup>[69]</sup>

(Continues)

TABLE 3 (Continued)

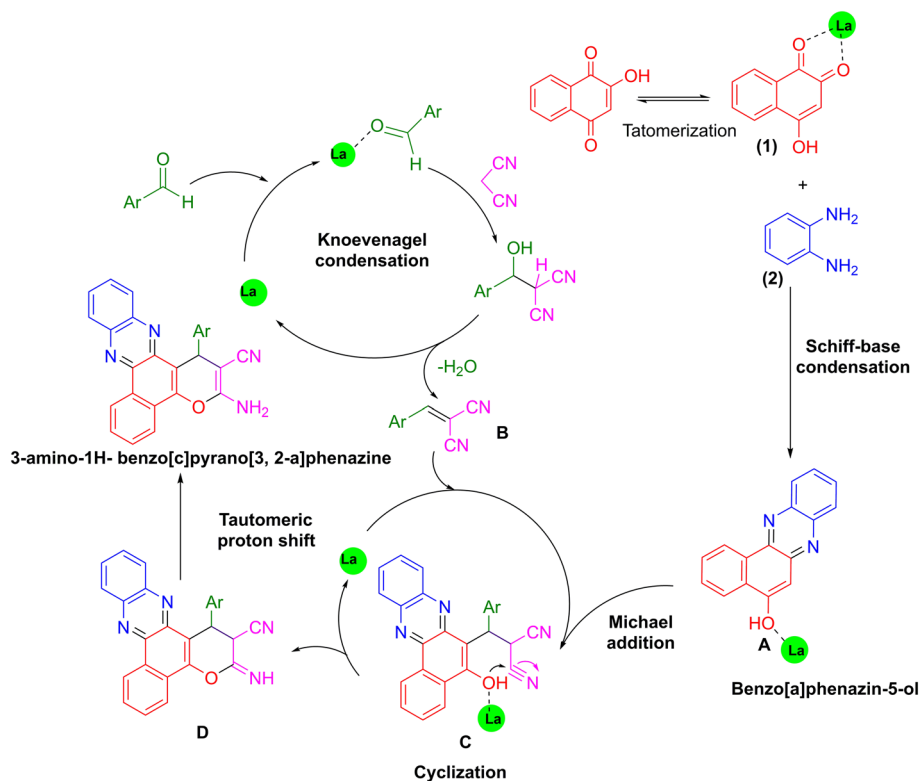
Entry	Aldehyde	Product	Time (h)	Yield <sup>a</sup> (%)	TON	TOF(h <sup>-1</sup> )	M.P °C	
							Measured	Literature
6			4	96	192	48	251–252	>250 <sup>[70]</sup>
7			2	87	174	87	280–282	281–283 <sup>[25]</sup>
8			4	98	196	49	282–284	282–285 <sup>[71]</sup>
9			4.5	92	184	40.88	274–276	275 <sup>[69]</sup>
10			5.5	94	188	34.18	250–252	>250 <sup>[72]</sup>

<sup>a</sup>Isolated yield.<sup>b</sup>Reaction conditions: -hydroxynaphthalene-1,4-dione (1 mmol) and benzene-1,2-diamine (1 mmol), aromatic aldehyde (1.0 mmol), malononitrile (1.5 mmol) and La@guanine@SBA-15 (0.5 mol %), in ethanol at reflux conditions.

(Scheme 3). As shown in Table 3, all the reactions were successfully performed and good to excellent yields have been achieved.

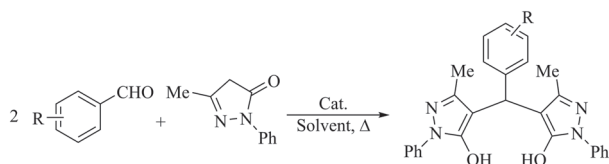
The suggested reaction mechanism for the described combination has been depicted in Scheme 4 based on the previously-reported reaction pathway.<sup>[15]</sup> Initially, the

**SCHEME 4** Proposed mechanism for the synthesis of 3-amino-1H-benzo[*c*]pyrano[3, 2-*a*]phenazines [Colour figure can be viewed at [wileyonlinelibrary.com](http://wileyonlinelibrary.com)]



intermediate **A** was formed from the Schiff-base condensation of benzene-1,2-diamine and 2-hydroxynaphthalene 1,4-dione in the presence of La-guanine@SBA-15 NPS. Sequentially, a possible intermediate **C** was formed via Michael addition of **B** with Benzo[*a*]phenazin-5-ol (intermediate **B** is formed via the Knoevenagel condensation of aldehyde with malononitrile in the presence of La-guanine@SBA-15 NPS). In the next step, intermolecular cyclization of intermediate **C** produced intermediate **D**. Finally, a tautomeric proton shift produced the final 3-amino-1H-benzo[*c*]pyrano[3, 2-*a*]phenazines product (Scheme 4).

Moreover, the role of the catalyst for the synthesis of 4,4'-(arylmethylene)-bis-(3-methyl-1-phenyl-1H-pyrazol-5-ols) derivatives was examined. The synthesis of these products using the reaction between aldehydes and 3-methyl-1-phenyl-1H-pyrazol-5(4H)-one in the presence of La@guanine@SBA-15 is shown in Scheme 5.



**SCHEME 5** Optimization of the reaction condition for the preparation of 4,4'-(arylmethylene)-bis-(3-methyl-1-phenyl-1H-pyrazol-5-ols)

In order to optimize the reaction conditions, the reaction of 3-methyl-1-phenyl-1H-pyrazol-5(4H)-one (1 mmol) and para-chloro benzaldehyde (2 mmol) was selected as the model reaction and the sample reaction was considered in different conditions such as the amounts of the catalyst, temperatures and solvents (Scheme 5). The obtained results are in Table 4. At first, the effect of various amounts of the catalyst were examined. We find out that the reaction does not proceed in the absence of La@guanine@SBA-15 even after 48 hr (Table 4, entry 1) and, in the presence of 0.1 mol% of the catalyst, only 53% yield of the product was achieved (Table 4, entry 2). Also, the increase in the amount of the catalyst up to 0.5 mol% increased the product yields up to 95% (Table 4, entry 5). Afterwards, we have successfully explored the effect of the solvents and temperature on the progress of the reaction. The results showed that a good yield was obtained in ethanol at reflux condition (Table 4, entry 5). A lower yield was observed when the temperatures were decreased (Table 4, entries 10–13). Therefore, 0.5 mol% of the catalyst, ethanol as solvent and reflux condition were selected as the best reaction conditions for the synthesis of 4,4'-(arylmethylene)-bis-(3-methyl-1-phenyl-1H-pyrazol-5-ols) derivatives in the present of La@guanine@SBA-15.

For future investigations on the generality and scope of this protocol, various electron-donating and electron-withdrawing aldehydes were explored under optimized

**TABLE 4** Optimization of the reaction condition for the preparation of 4,4'-(arylmethylene)-bis-(3-methyl-1-phenyl-1H-pyrazol-5-ols)

Entry	Amount of Catalyst (mol%)	Solvent	Temperature (°C)	Time (min)	Yield <sup>a</sup> (%)
1	-	Ethanol	Reflux	2 day	Trace
2	0.1	Ethanol	Reflux	30	53
3	0.2	Ethanol	Reflux	30	63
4	0.4	Ethanol	Reflux	30	84
5	0.5	Ethanol	Reflux	30	95
6	0.5	Acetonitrile	Reflux	30	87
7	0.5	DMSO	100	30	83
8	0.5	PEG-400	100	30	64
9	0.5	DMF	100	30	81
10	0.5	Ethanol	25	30	b
11	0.5	Ethanol	60	30	63
12	0.5	Ethanol	70	30	84
13	0.5	Ethanol	75	30	87

<sup>a</sup>Isolated yield.<sup>b</sup>No reaction.

reaction conditions (Scheme 6). As shown in Table 5, the obtained results show that all the products were obtained in high to excellent yields.

The suggested reaction mechanism for the described combination via tandem Knoevenagel–Michael reaction in the presence of La-guanine@SBA-15 nanocatalyst has been depicted in Scheme 7 based on the previously-reported reaction pathway.<sup>[77]</sup> Initially, the intermediate **III** was formed from the Knoevenagel condensation of aldehyde and Pyrazolone in the presence of La-guanine@SBA-15 nanocatalyst. Sequentially, a possible intermediate **IV** was formed via Michael addition of the second mol of Pyrazolone with the intermediate **III** in order to give bis (pyrazolyl)methanes.

## 5 | CATALYST REUSABILITY

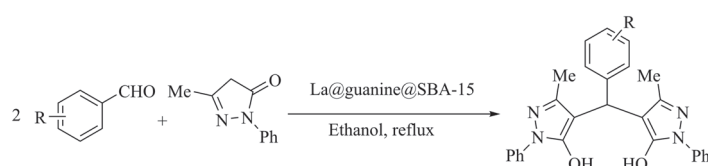
To check the reusability of La@guanine@SBA-15, we examined the reaction between 3-methyl-1-phenyl-1H-pyrazol-5(4H)-one (1 mmol) and para-chloro benzaldehyde (2 mmol) for the synthesis of 4,4'-(arylmethylene)-bis-(3-methyl-1-phenyl-1H-pyrazol-5-ols) derivatives (column a), and also, 2-hydroxynaphthalene-1,4-dione (1 mmol), benzene-1,2-diamine (1 mmol), para-chloro

benzaldehyde (1.0 mmol) and malononitrile (1.5 mmol) for the synthesis of benzo[c]pyrano[3,2-a]phenazine derivatives (column b) under the optimized reaction conditions. After completion of the reaction, the solid catalyst was separated by simple filtration, washed by ethanol and acetone and, then, subjected to the next run. The catalyst has been reused up to over five runs without any significant loss of its catalytic activity (Figure 8).

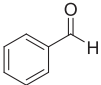
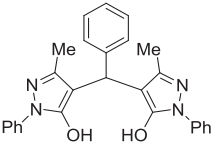
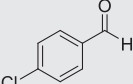
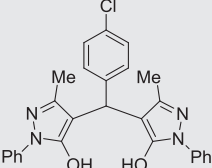
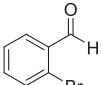
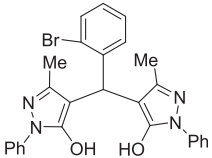
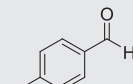
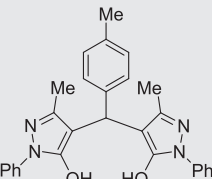
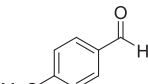
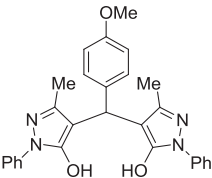
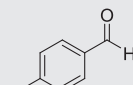
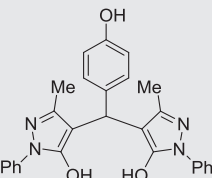
Besides, in order to examine the stability of the catalyst after recycling, the recycled catalyst has been characterized by FT-IR and SEM techniques. These characterizations confirmed that the recovered catalyst is in good agreement with the fresh catalyst. These characterizations are strong evidences for the high stability of La-guanine-Sba-15 after recycling.

FT-IR spectrums of the recycled catalyst are shown in Figure 9. The results show that a good agreement can be observed for FT-IR of the fresh La@guanine@SBA-15 (Figure 9a) and the recycled catalyst (Figure 9b). In this sense, Figure 9 illustrates good stability of La@guanine@SBA-15 after recycling.

The SEM image of the recycled catalyst is shown in Figure 10 in which the particles of the recovered catalyst were observed between 15–20 nm with homogeneous size and morphology. SEM image of the recycled catalyst is in

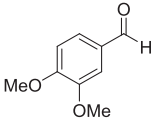
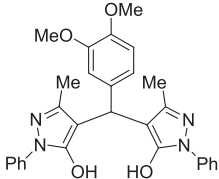
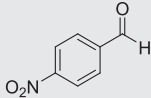
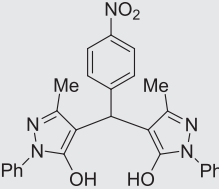
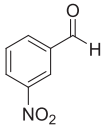
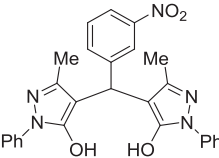
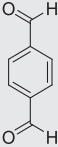
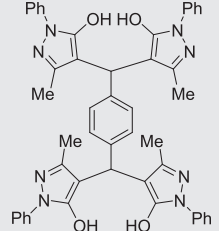
**SCHEME 6** Synthesis of 4,4'-(arylmethylene)-bis-(3-methyl-1-phenyl-1H-pyrazol-5-ols) derivatives in the presence of La@guanine@SBA-15

**TABLE 5** Synthesis of 4,4'-(arylmethylene)-bis-(3-methyl-1-phenyl-1H-pyrazol-5-ols) derivatives catalyzed by La@guanine@SBA-15<sup>a</sup>

Entry	Aldehyde	Product	Time (min)	Yield (%) <sup>b</sup>	TON	TOF (min <sup>-1</sup> )	M.P. °C	
							Measured	Literature
1			40	98	196	4.9	169–171	170–172 <sup>[73]</sup>
2			30	95	190	6.33	212–214	213–215 <sup>[74]</sup>
3			30	95	190	6.33	198–200	198–200 <sup>[75]</sup>
4			45	94	188	4.17	200–203	202–204 <sup>[73]</sup>
5			55	87	174	3.16	172–174	173–175 <sup>[74]</sup>
6			50	88	176	3.52	153–155	153–155 <sup>[74]</sup>

(Continues)

TABLE 5 (Continued)

Entry	Aldehyde	Product	Time (min)	Yield (%) <sup>b</sup>	TON	TOF (min <sup>-1</sup> )	M.P °C	
							Measured	Literature
7			90	93	186	2.06	194–197	194–196 <sup>[74]</sup>
8			25	91	182	7.28	226–228	225–227 <sup>[75]</sup>
9			35	89	178	5.08	150–152	151–153 <sup>[76]</sup>
10			120	84	168	1.4	214–216	214–216 <sup>[75]</sup>

<sup>a</sup>Reaction conditions: 3-methyl-1-phenyl-1H-pyrazol-5(4H)-one (1 mmol), aldehyde (2 mmol), La@guanine@SBA-15 (0.5 mol %), in ethanol at reflux condition,

<sup>b</sup>Isolated yield.

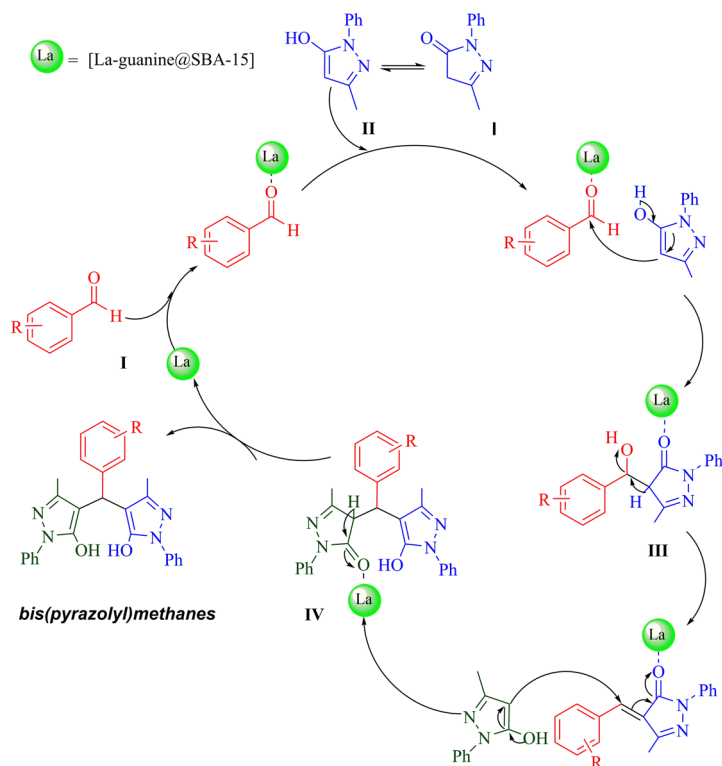
good agreement with SEM image of the fresh catalyst (Figure 5). Therefore, size and shape of the catalyst have not been changed after recycling.

## 6 | HOT FILTRATION TEST

Moreover, hot filtration test was performed in order to prove that the La was not leaching out from the solid catalyst during the organic reactions. Accordingly, the synthesis of 3-amino-1-(4-chlorophenyl)-1H-benzo[a]

pyrano[2,3-c]phenazine-2-carbonitrile and 4,4'-((4-chlorophenyl)methylene)bis(3-methyl-1-phenyl-1H-pyrazol-5-ol) in the presence of La@guanine@SBA-15 was performed under the optimal reaction conditions. After half-time of the reactions, they were terminated, and the corresponding products were obtained in 57 and 45% of yields, respectively. Afterwards, both of the reactions were repeated, then, at the half-time of the reaction, the catalyst was separated by simple filtration from the reaction mixture and, finally, the filtrate was allowed to react further. We found out that only a trace conversion

**SCHEME 7** Proposed mechanism for the synthesis of 4,4'-(arylmethylene)-bis-(3-methyl-1-phenyl-1H-pyrazol-5-ols) [Colour figure can be viewed at wileyonlinelibrary.com]



(< 3 and 4% respectively) of the tandem Knoevenagel condensation–Michael addition–cyclization reactions was observed upon heating the catalyst-free solution for other half time of the reaction. In addition, the exact amount of La, in the recovered catalyst, was obtained by ICP-OSE as  $1.30 \times 10^{-3} \text{ mol g}^{-1}$ .

## 7 | LEACHING TEST

In order to consider the leaching of La into the reaction media, ICP-AES analysis was performed. Besides, the La

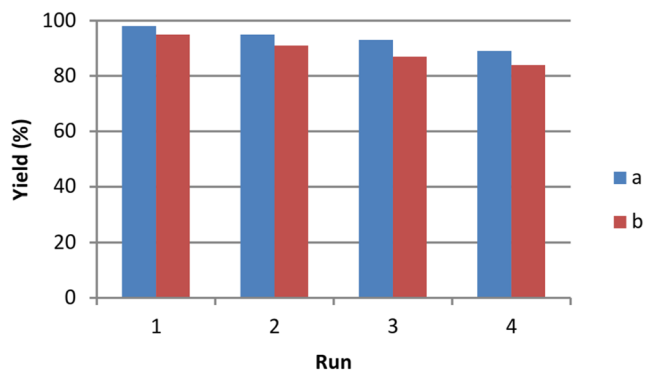


**FIGURE 8** Reuse of the La@guanine@SBA-15 for the synthesis of 4,4'-(arylmethylene)-bis-(3-methyl-1-phenyl-1H-pyrazol-5-ols) derivatives (column a) and benzo[c]pyrano[3,2-a]phenazine derivatives (column b) [Colour figure can be viewed at wileyonlinelibrary.com]

content in the reaction media in the synthesis of 3-amino-1-(4-chlorophenyl)-1H-benzo[a]pyrano[2,3-c]phenazine-2-carbonitrile and 4,4'-((4-chlorophenyl)

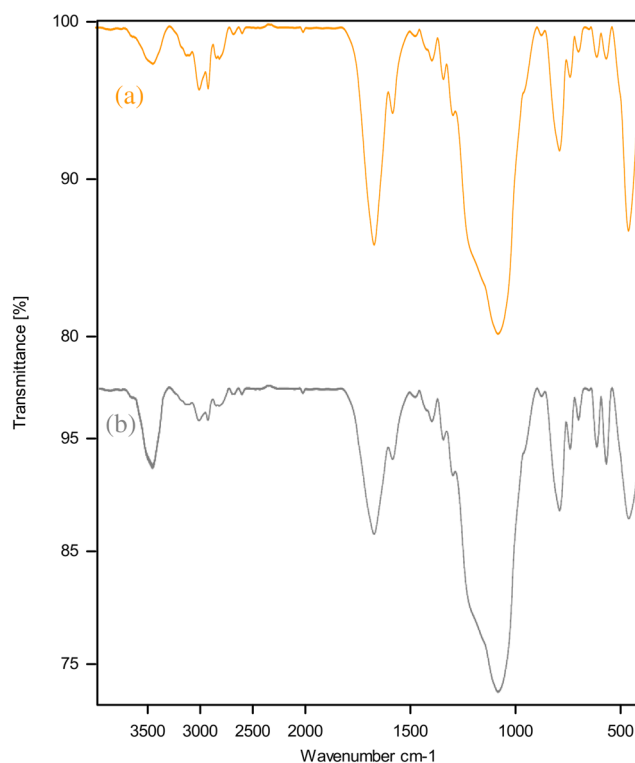


**FIGURE 9** FT-IR spectra of (a) La@guanine@SBA-15 and (b) recovered La@guanine@SBA-15 catalyst [Colour figure can be viewed at wileyonlinelibrary.com]

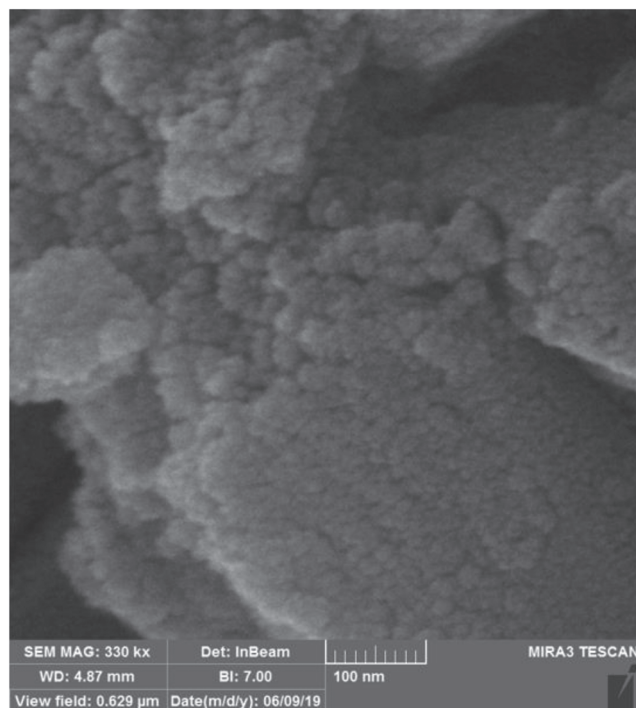


**FIGURE 10** SEM image of recovered La@guanine@SBA-15 nanocatalyst

methylene)bis(3-methyl-1-phenyl-1H-pyrazol-5-ol) was found to be 0.79 and 0.67%, respectively. The results show that the leaching of La into the reaction media is negligible.

## 8 | COMPARISON

In order to demonstrate the superiority of our catalyst to other reported catalysts for the synthesis of bis(pyrazolyl)methanes (Table 5) and polyhydroquinolines (Table 6), using p-Clbenzaldehyde, as the representative example, they were compared to the best of the well-known data from the literature as outlined in the Table 6 and 7, respectively. As it can be seen in this Table 6 & 7, this new method was better than the other catalysts in terms of reaction temperature, time and yield factors.

## 9 | CONCLUSION

Herein, we have utilized La@guanine@SBA-15 as a green and heterogeneous catalyst for the one pot, domino multi-component synthesis of benzo [a] pyrano [2, 3-c]

**TABLE 6** Comparison results of efficiency of La@guanine@SBA-15 in the synthesis of 4,4'-((4-chlorophenyl)methylene) bis(3-methyl-1-phenyl-1H-pyrazol-5-ol) with other catalysts reported in the literature

Entry	Catalyst	Conditions	Time (min)	Yield (%) <sup>a</sup>	TON	TOF (min <sup>-1</sup> )	Ref.
1	aspirin	EtOH/H <sub>2</sub> O, 60 °C	30	92	6.1	0.20	[78]
2	AP-SiO <sub>2</sub>	CH <sub>3</sub> CN, r.t	5	97	3.2	0.64	[79]
3	DCDBTSD	Solvent-free, 80 °C	40	80	8.0	0.20	[80]
4	CuFe <sub>2</sub> O <sub>4</sub>	Solvent-free, 80 °C	8	96	24.0	3.00	[81]
5	[Pyridine-SO <sub>3</sub> H]Cl	Solvent-free, 50 °C	8	94	94	11.75	[82]
6	SASPSPE	EtOH, Reflux	132	85	25	0.18	[83]
7	Ni-guanidine@MCM-41 NPs	Acetonitrile, 80 °C	20	90	11.2	0.56	[77]
8	La@guanine@SBA-15	EtOH, Reflux	30	95	190	6.33	This work

<sup>a</sup>Isolated yield.

**TABLE 7** Comparison results of efficiency of La@guanine@SBA-15 in the synthesis of 3-amino-1-(4-chlorophenyl)-1H-benzo[a]pyrano[2,3-c]phenazine-2-carbonitrile with other catalysts reported in the literature

Entry	Catalyst	Conditions	Time (min)	Yield (%) <sup>a</sup>	Ref.
1	DABCO	EtOH, Reflux	300	91	[72]
2	Nano CuO	Solvent -Free, 75 °C	7	94	[84]
3	1-butyl-3-methylimidazolium hydroxide	Solvent -Free, 75 oC	6	94	[69]
4	FeAl <sub>2</sub> O <sub>4</sub> (Hercynite)	PEG, 90 °C	180	90	[15]
5	Ni-Gly-isatin@boehmite	PEG, 80 °C	120	90	[28]
6	La@guanine@SBA-15	EtOH, Reflux	180	98	This work

<sup>a</sup>Isolated yield.

phenazine and the synthesis of 4,4'-(arylmethylene)-bis-(3-methyl-1-phenyl-1H-pyrazol-5-ols) derivatives. The solid catalyst was characterized by TGA, XRD, FT-IR, EDS, SEM, MAP and BET techniques. This procedure has the advantages of minimizing the chemical wastes, being safe and environmentally-friendly, having mild reaction conditions, ease of separation and non-toxic and reusable catalyst and also giving the products in high yields within short reaction times.

## ACKNOWLEDGMENTS

This work was supported by the Iran National Science Foundation and research facilities of Ilam University, Ilam, Iran.

## ORCID

Mohsen Nikoorazm  <https://orcid.org/0000-0002-4013-0868>

Masoud Mohammadi  <https://orcid.org/0000-0002-1043-3470>

## REFERENCES

- [1] L. Reguera, D. G. Rivera, *Chem. Rev.* **2019**, *119*, 9836.
- [2] C. G. Neochoritis, T. Zhao, A. Dömling, *Chem. Rev.* **2019**, *119*, 1970.
- [3] M. Kazemi, M. Mohammadi, *Appl. Organometal Chem.* **2019**, e5400. (Article in press), <https://doi.org/10.1002/aoc.5400>
- [4] L. Zhang, J. Dong, X. Xu, Q. Liu, *Chem. Rev.* **2016**, *116*, 287.
- [5] T. Tamoradi, S. M. Mousavi, M. Mohammadi, *New J. Chem.* **2020**. (Article in Press), <https://doi.org/10.1039/C9NJ05468E>
- [6] C. M. R. Volla, I. Atodiresei, M. Rueping, *Chem. Rev.* **2014**, *114*, 2390.
- [7] T. Tamoradi, H. Veisi, B. Karmakar, J. Gholami, *Mater. Sci. Eng. C* **2020**, *107*, 110260.
- [8] B. H. Rotstein, S. Zaretsky, V. Rai, A. K. Yudin, *Chem. Rev.* **2014**, *114*, 8323.
- [9] M. A. Mironov, *Russ. J. Gen. Chem.* **2010**, *80*, 2628.
- [10] A. Dömling, W. Wang, K. Wang, *Chem. Rev.* **2012**, *112*, 3083.
- [11] J. H. Kim, Y. O. Ko, J. Bouffard, S. Lee, *Chem. Soc. Rev.* **2015**, *44*, 2489.
- [12] F. Feizpour, M. Jafarpour, A. Rezaeifard, *Catal. Letters* **2018**, *148*, 30.
- [13] B. Atashkar, M. A. Zolfigol, S. Mallakpour, *Mol. Catal.* **2018**, *452*, 192.
- [14] A. Ghorbani-Choghamarani, M. Mohammadi, T. Tamoradi, M. Ghadermazi, *Polyhedron* **2019**, *158*, 25.
- [15] A. Ghorbani-Choghamarani, M. Mohammadi, L. Shiri, Z. Taherinia, *Res. Chem. Intermed.* **2019**, *45*, 5705.
- [16] H. Alinezhad, M. Tarahomi, B. Maleki, A. Amiri, *Appl. Organomet. Chem.* **2019**, 33.
- [17] R. Tayebee, M. Fattahi Abdizadeh, N. Erfaninia, A. Amiri, M. Baghayeri, R. M. Kakhki, B. Maleki, E. Esmaili, *Appl. Organomet. Chem.* **2019**.
- [18] B. Maleki, R. Tayebee, Z. Sepehr, M. Kermanian, *Acta Chim. Slov.* **2012**, *59*, 814.
- [19] R. Tayebee, A. Pejhan, H. Ramshini, B. Maleki, N. Erfaninia, Z. Tabatabaie, E. Esmaeili, *Appl. Organomet. Chem.* **2018**, 32.
- [20] M. Rouhani, A. Ramazani, *J. Iran. Chem. Soc.* **2018**, *15*, 2375.
- [21] I. Khan, A. Ibrar, N. Abbas, A. Saeed, *Res. Chem. Intermed.* **2016**, *42*, 5147.
- [22] R. Nouri, S. Abedi, A. Morsali, *J. Iran. Chem. Soc.* **2017**, *14*, 1601.
- [23] S. Haghshenas Kashani, M. Moghadam, S. Tangestaninejad, V. Mirkhani, I. Mohammadpoor-Baltork, *Catal. Letters* **2018**, *148*, 1110.
- [24] F. Shirini, M. Seddighi, M. Mazloumi, M. Makhsoos, M. Abedini, *J. Mol. Liq.* **2015**, *208*, 291.
- [25] S. L. Wang, F. Y. Wu, C. Cheng, G. Zhang, Y. P. Liu, B. Jiang, F. Shi, S. J. Tu, *ACS Comb. Sci.* **2011**, *13*, 135.
- [26] Y. Lu, L. Wang, X. Wang, T. Xi, J. Liao, Z. Wang, F. Jiang, *Eur. J. Med. Chem.* **2017**, *135*, 125.
- [27] H. Naeimi, M. F. Zarabi, *RSC Adv.* **2019**, *9*, 7400.
- [28] A. Ghorbani-Choghamarani, R. Sahraei, Z. Taherinia, *Res. Chem. Intermed.* **2019**, *45*, 3199.
- [29] M. A. Ashraf, Z. Liu, W.-X. Peng, *Appl. Organomet. Chem.* **2019**, *34*, e5260.
- [30] H. Xie, H. Liu, M. Wang, H. Pan, C. Gao, *Appl. Organomet. Chem.* **2019**, *34*, e5256.
- [31] N. Guttenberger, W. Blankenfeldt, R. Breinbauer, *Bioorganic Med. Chem.* **2017**, *25*, 6149.
- [32] K. Verma, Y. K. Tailor, S. Khandelwal, M. Agarwal, E. Rushell, Y. Kumari, K. Awasthi, M. Kumar, *RSC Adv.* **2018**, *8*, 30430.
- [33] T. Tomasic, L. Masic, *Curr. Med. Chem.* **2009**, *16*, 1596.
- [34] R. Ranjith Kumar, S. Perumal, J. C. Menéndez, P. Yogeewari, D. Sriram, *Bioorganic Med. Chem.* **2011**, *19*, 3444.
- [35] A. M. El-Agrody, A. M. Fouda, E. Khatatb, *Med. Chem. Res.* **2013**, *22*, 6105.
- [36] A. Chaudhary, J. M. Khurana, *Res. Chem. Intermed.* **2018**, *44*, 1045.
- [37] A. Yazdani-Elah-Abadi, R. Mohebat, M. T. Maghsoodlou, R. Heydari, *Polycyclic Aromat. Compd.* **2018**, *38*, 92.
- [38] F. Dickens, H. McIlwain, *Biochem. J.* **1938**, *32*, 1615.
- [39] S. Abbasi Pour, A. Yazdani-Elah-Abadi, M. Afradi, *Appl. Organomet. Chem.* **2017**, *31*, e3791.
- [40] A. Mehmood, H. Ghafar, S. Yaqoob, U. F. Gohar, B. Ahmad, *J. Dev. Drugs* **2017**, 06.
- [41] M. Eslami, M. G. Dekamin, L. Motlagh, A. Maleki, *Green Chem. Lett. Rev.* **2018**, *11*, 36.
- [42] V. Chaudhary, S. Sharma, *J. Porous Mater.* **2017**, *24*, 741.
- [43] R. Huirache-Acuña, R. Nava, C. Peza-Ledesma, J. Lara-Romero, G. Alonso-Núñez, B. Pawelec, E. Rivera-Muñoz, *Materials (Basel)* **2013**, *6*, 4139.
- [44] M. Y. Huang, X. X. Han, C. T. Hung, J. C. Lin, P. H. Wu, J. C. Wu, S. B. Liu, *J. Catal.* **2014**, *320*, 42.
- [45] M. Balaraju, P. Nikhitha, K. Jagadeeswaraiiah, K. Srilatha, P. S. Sai Prasad, N. Lingaiah, *Fuel Process. Technol.* **2010**, *91*, 249.
- [46] Y. Choi, A. Sinha, J. Im, H. Jung, J. Kim, *ACS Appl. Mater. Interfaces* **2019**, *11*, 15764.
- [47] E. M. Björk, *J. Chem. Educ.* **2017**, *94*, 91.
- [48] M. Mohammadi, A. Ghorbani-Choghamarani, *New J. Chem.* **2020**. (Article In press), <https://doi.org/10.1039/C9NJ05325E>

- [49] N. Lashgari, A. Badiei, G. M. Ziarani, *Nano. Chem. Res.* **2016**, *1*, 127.
- [50] A. Kavosi, F. Faridbod, M. R. Ganjali, *Int. J. Environ. Res.* **2015**, *9*, 247.
- [51] Y. Qin, Y. Wang, H. Wang, J. Gao, Z. Qu, *Procedia Environ. Sci.* **2013**, *18*, 366.
- [52] L. Wang, H. He, C. Zhang, L. Sun, S. Liu, R. Yue, *J. Appl. Microbiol.* **2014**, *116*, 1106.
- [53] C. B. Yu, C. Wei, J. Lv, H. X. Liu, L. T. Meng, *Express Polym. Lett.* **2012**, *6*, 783.
- [54] J. Mondal, P. Borah, A. Modak, Y. Zhao, A. Bhaumik, *Org. Process Res. Dev.* **2014**, *18*, 257.
- [55] G. R. Wilson, A. Dubey, *J. Chem. Sci.* **2016**, *128*, 1285.
- [56] Q. Pu, M. Kazemi, M. Mohammadi, *Mini. Rev. Org. Chem.* **2019**, *16*, 5775.
- [57] L. Chen, A. Noory Fajer, Z. Yessimbekov, M. Kazemi, M. Mohammadi, *J. Sulfur Chem.* **2019**, *40*, 451.
- [58] A. Ghorbani-Choghamarani, M. Mohammadi, R. H. E. Hudson, T. Tamoradi, *Appl. Organomet. Chem.* **2019**, *33*, e4977.
- [59] A. Ghorbani-Choghamarani, M. Mohammadi, Z. Taherinia, *J. Iran. Chem. Soc.* **2019**, *16*, 411.
- [60] M. Kazemi, S. M. Nasr, Z. Chen, M. Mohammadi, *Mini. Rev. Org. Chem.* **2019**, *16*, (Article in press). <https://doi.org/10.2174/1570193X166661907>
- [61] J. Li, X. Bai, H. Lv, *Microporous Mesoporous Mater.* **2019**, *275*, 69.
- [62] S. Feng, B. Zhao, Y. Liang, L. Liu, J. Dong, *Ind. Eng. Chem. Res.* **2019**, *58*, 2661.
- [63] C. Ji, Y. Wang, N. Zhao, *Appl. Surf. Sci.* **2019**, *481*, 337.
- [64] C. C. Chong, H. D. Setiabudi, A. A. Jalil, *Int. J. Hydrogen Energy* **2019**.
- [65] M. Prabhu, M. Manikandan, P. Kandasamy, P. R. Kalaivani, N. Rajendiran, T. Raja, *ACS Omega* **2019**, *4*, 3500.
- [66] L. Hosseini, R. Moreno-Atanasio, F. Neville, *Langmuir* **2019**, *35*, 7896.
- [67] J. Li, Y. Tang, Z. Li, X. Ding, B. Yu, L. Lin, *ACS Appl. Mater. Interfaces* **2019**, *11*, 18808.
- [68] H. L. Chiang, T. N. Wu, L. X. Zeng, *Microporous Mesoporous Mater.* **2019**, *279*, 286.
- [69] H. R. Shaterian, M. Mohammadnia, *J. Mol. Liq.* **2013**, *177*, 162.
- [70] J. Gao, M. Chen, X. Tong, H. Zhu, H. Yan, D. Liu, W. Li, S. Qi, D. Xiao, Y. Wang, Y. Lu, F. Jiang, *Comb. Chem. High Throughput Screening* **2015**, *18*, 960.
- [71] A. Y. E. Abadi, M. T. Maghsoodlou, R. Heydari, R. Mohebat, *Res. Chem. Intermed.* **2016**, *42*, 1227.
- [72] A. Hasaninejad, S. Firoozi, *Divers.* **2013**, *17*, 499.
- [73] K. Niknam, S. Mirzaee, P. Gulf, *Synth. Commun.* **2011**, *41*, 37.
- [74] M. Keshavarz, M. Vafaei-Nezhad, *Catal. Letters* **2016**, *146*, 353.
- [75] M. Makvandi, F. A. Dil, A. Malekzadeh, M. Baghernejad, K. Niknam, *Iran. J. Catal.* **2013**, *3*, 221.
- [76] M. Baghernejad, K. Niknam, *Int. J. Chem.* **2012**, *4*, 52.
- [77] H. Filian, A. Ghorbani-Choghamarani, E. Tahanpesar, *J. Iran. Chem. Soc.* **2019**.
- [78] M. Fatahpour, F. Noori Sadeh, N. Hazeri, M. T. Maghsoodlou, M. Lashkari, *J. Iran. Chem. Soc.* **2017**, *14*, 1945.
- [79] S. Sobhani, A.-R. Hasaninejad, M. F. Maleki, Z. P. Parizi, *Synth. Commun.* **2012**, *42*, 2245.
- [80] A. Khazaei, F. Abbasi, A. R. Moosavi-Zare, *New J. Chem.* **2014**, *38*, 5287.
- [81] R. Khalifeh, R. Shahmoridi, M. Rajabzadeh, *Catal. Letters* **2019**, *149*, 2864.
- [82] A. R. Moosavi-Zare, Z. Asgari, A. Zare, M. A. Zolfigol, *Sci. Iran.* **2015**, *22*, 2254.
- [83] S. Tayebi, M. Baghernejad, D. Saberi, K. Niknam, *Chinese J. Catal.* **2011**, *32*, 1477.
- [84] H. R. Shaterian, F. Moradi, M. Mohammadnia, *Comptes Rendus Chim.* **2012**, *15*, 1055.

**How to cite this article:** Nikoorazm M, Khanmoradi M, Mohammadi M. Guanine-La complex supported onto SBA-15: A novel efficient heterogeneous mesoporous nanocatalyst for one-pot, multi-component Tandem Knoevenagel condensation–Michael addition–cyclization Reactions. *Appl Organometal Chem.* 2020;e5504. <https://doi.org/10.1002/aoc.5504>